# Macroscopic Evidence of Soliton Formation in Multiterawatt Laser-Plasma Interaction

M. Borghesi,[1] S. Bulanov,[2] D. H. Campbell,[3] R. J. Clarke,[4] T. Zh. Esirkepov,[5] M. Galimberti,[6] L. A. Gizzi,[6] A. J. MacKinnon,[7] N. M. Naumova,[8] F. Pegoraro,[9] H. Ruhl,[8] A. Schiavi,[3] and O. Willi[10]

[1]*Department of Pure & Applied Physics, Queen's University, Belfast, United Kingdom*
[2]*General Physics Institute, RAS, Moscow, Russia*
[3]*The Blackett Laboratory, Imperial College, London, United Kingdom*
[4]*Central Laser Facility, Rutherford Appleton Laboratory, Chilton, United Kingdom*
[5]*Moscow Institute of Physics and Technology, Dolgoprudny, Russia*
[6]*Istituto di Fisica Atomica e Molecolare-C.N.R., Pisa, Italy*
[7]*Lawrence Livermore National Laboratory, Livermore, California 94550*
[8]*Max-Born Institut für Quantenoptik, Berlin, Germany*
[9]*Department of Physics, Pisa University and IFNM, Pisa, Italy*
[10]*Institut für Laser-und Plasmaphysik, Heinrich-Heine-Universität, Düsseldorf, Germany*

A novel physical phenomenon has been observed following the interaction of an intense ($10^{19}$ W/cm$^2$) laser pulse with an underdense plasma. Long-lived, macroscopic bubblelike structures have been detected through the deflection that the associated electric charge separation causes in a proton probe beam. These structures are interpreted as the remnants of a cloud of relativistic solitons generated in the plasma by the ultraintense laser pulse. This interpretation is supported by an analytical study of the soliton cloud evolution, by particle-in-cell simulations, and by a reconstruction of the proton-beam deflection.

Experiments studying the interaction of ultraintense, ultrashort laser pulses with plasmas provide unique laboratory conditions for the study of the collective nonlinear dynamics of a macroscopic system in the relativistic regime. In addition, investigating the structure of the nonlinear coherent modes in the wake of a short laser pulse is of great practical interest as it shows how the laser pulse energy can be transferred to the electromagnetic fields in the plasma and to fast particles. Coherent structures, such as solitons (see [1] and references therein) and vortices, are fundamental features of this nonlinear interaction. Indeed, analytical and numerical results have shown that low-frequency, slowly propagating, subcycle solitons can be generated in the interaction of ultrashort ultraintense laser pulses with underdense plasmas. A significant fraction of the laser pulse energy can be trapped in these structures in the form of electromagnetic energy oscillating at a frequency smaller than the Langmuir frequency $\omega_{pe}$ of the surrounding plasma. The typical size of these solitons is of the order of the collisionless electron skin depth $d_e = c/\omega_{pe}$. The fields inside the solitons consist of synchronously oscillating electric and magnetic fields plus a steady electrostatic field which arises from the charge separation as electrons are pushed outward by the ponderomotive force of the oscillating fields. As yet no direct experimental proof of soliton generation in the laser plasma interaction has been obtained. Indeed, the experimental detection of such structures poses phenomenal challenges due to their microscopic scale and to their transient nature.

In this Letter we report the experimental observation of bubblelike structures in proton images of laser-produced plasmas which we interpret as the macroscopic remnants [2] of solitons formed in the interaction with the ultraintense pulse. The observed structures correspond to localized depletion regions in the cross section of a transverse-propagating proton probe beam. We believe that these are the first experimental observations of quasineutral cavitated postsolitons. The bubbles appear as the protons are deflected away by the localized electric field in correspondence of the cavitated areas. This interpretation is supported by computational and analytical results.

The experiment was carried out at the Rutherford Appleton Laboratory employing the VULCAN Nd:glass laser operating in the chirped pulse amplification mode (CPA). The VULCAN CPA pulse was split in two separate 1 ps, 1 $\mu$m, 20 J pulses (CPA$_1$ and CPA$_2$) which were focused onto separate targets in a $10-15$ $\mu$m FWHM focal spot giving an average intensity of about $10^{19}$ W/cm$^2$. The experimental arrangement is shown schematically in Fig. 1a. The CPA$_1$ pulse was used as the main interaction pulse and focused into a preformed plasma. The plasmas were produced by exploding thin plastic foils (0.3 $\mu$m thick) with two 1 ns, 0.527 $\mu$m laser pulses at a total irradiance of about $5 \times 10^{14}$ W/cm$^2$. The delay between plasma formation and interaction was typically 1 ns. The CPA$_2$ pulse was focused onto a 3 $\mu$m Al foil in order to produce a beam of multi-MeV protons, which were used as a transverse particle probe of the interaction region. This is a diagnostic scheme for detection of electric fields in plasmas recently proposed as proton imaging [3]. The delay between the two CPA pulses could be varied optically. As observed in several experiments under these
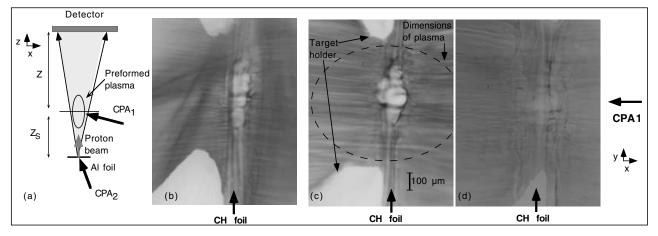
FIG. 1.   (a) Experimental arrangement. (b), (c), (d) Proton images of the preformed plasma taken with 6−7 MeV protons, respectively: (b) 25 ps; (c) 45 ps; (d) 95 ps after the $CPA_1$ interaction. The scale refers to dimensions in the object plane. The dashed line indicates the dimensions of the preformed plasma defined by $n \approx 0.01 n_{cr}$ (at $\lambda = 1\ \mu$m).

irradiation conditions proton bursts are emitted (in this particular case with energies up to 10 MeV and temperature 1.5 MeV) normal to the back surface of the target with small angular divergence and with ps duration [4–6]. As the proton source is small, the proton probe could be used in a point-projection imaging arrangement with the magnification determined by $1 + Z/Z_s$, where $Z = 2$ cm and $Z_s = 2$ mm are, respectively, the object-to-detector and object-to-source distances [3]. The spatial resolution was determined by the apparent size of the proton source, which has been found to be smaller than 10 $\mu$m via penumbral edge measurements, while the temporal resolution was found to be better than 5 ps [7].

The proton detector employed consisted of a stack of several layers of radiochromic (RC) film [8], namely MD-55 GafChromic, with a 25 $\mu$m Al filter placed in front of the first layer of film. The RC film (RCF) consisted of 270 $\mu$m thick plastic containing a double layer of organic dye, which reacts to ionizing radiation. The diagnostic use of stacks of RCF for obtaining spectrally selected information on the equivalent dose of the protons stopped is described in Refs. [3,6]. Basically each RC film layer of the stack contains information relating mainly to a particular, narrow range of proton energies. A further, low energy fraction of the CPA pulse was frequency quadrupled and used as a transverse optical probe, alternatively to the particle probe. Interferometry was performed along this line using a modified Nomarsky interferometer, which allowed density characterization of the preformed plasma. The peak density of the plasma was inferred to be $(0.1-0.2)n_{\mathrm{crit}}$ at $\lambda = 1\ \mu$m from self-consistent plasma expansion models [9] and its longitudinal extension was of the order of a mm. By adjusting the delay between the $CPA_1$ and $CPA_2$ pulses, it was possible to probe the plasma with the proton beam at different times following the interaction. The main feature observed in the proton images (i.e., the proton-beam intensity cross section after propagation through the plasma) was the onset of several bubblelike structures following the interaction. Proton

images of the plasma obtained with 6–7 MeV protons and recorded, in different shots, at various delays after the interaction are also shown in Fig. 1: 5–6 bubblelike structures are clearly visible at the center of the plasma in Figs. 1b and 1c corresponding to delays of 25 and 45 ps after the $CPA_1$ interaction. In particular, a large structure with radius of approximately 50 $\mu$m is seen at the center of Fig. 1c, with the other 5 smaller structures tightly packed around it. The structures are first observed in coincidence with the interaction. No structures have been clearly observed at later times, as can be seen in Fig. 1d taken 100 ps after the $CPA_1$ interaction. The "bubbles" correspond to unexposed regions of the RCF, i.e., regions of the proton-beam cross section from which protons have been evacuated. As the aerial density of the matter crossed by the beam is insignificant compared to the stopping range of the protons employed, it is reasonable to assume that the bubbles are observed in correspondence of plasma regions where localized electric field, with a component transverse to the proton propagation direction, are present. The region where the bubbles are present extend for about 300 $\mu$m in the transverse direction and for about 150 $\mu$m in the longitudinal direction. They are therefore observed even far away from the interaction axis and the vacuum focal spot region. It should be noted that in similar interaction conditions, breakup of the laser beam in several filaments diverging at wide angles has been observed [10]. This causes fractions of the laser energy to be spread as far as 150 $\mu$m from the propagation axis in the plasma central plane. In the presence of this filamentary behavior, no efficient channel formation process via Coulomb explosion following the interaction was observed. It is therefore reasonable to assume that the spatial scale of the area occupied by the bubbles in the proton images is consistent with the dimension of the turbulent region left by the laser pulse in the central part of the plasma. The horizontal striations seen in Fig. 1b are likely to be due to a different phenomenon, namely electromagnetic instabilities initiated by the return current

of hot electrons ejected from the focal spot region during the interaction [3].

We believe that these observations are consistent with structures (postsolitons) formed by the expansion and merging of several solitons, and we support this assumption with analytical and computational modeling. As shown in Ref. [2], on time scales longer than $(m_i/m_e)^{1/2}\omega_{pe}^{-1}$ the nature of the slow propagating subcycle solitons described in [1], changes because ions start to expand. As a consequence, a void forms in the ion density and the soliton is changed into a radially expanding postsoliton structure that is largely quasineutral. As the hole expands, the amplitude and the frequency $\omega_s$ of the electromagnetic field decrease. From the adiabatic invariant $\int \mathbf{E}^2 \, dV / \omega_s = $ const we see that the electromagnetic field amplitude decreases as $E \sim 1/R^2$. Using a snowplow model, the characteristic expansion time of the postsoliton is found to be given by $\tau = \sqrt{6\pi R_0^2 n_0 m_i / \langle \mathbf{E}_0^2 \rangle}$ with $n_0$ the plasma density and $R_0 \approx d_e$ and $\mathbf{E}_0^2/8\pi$ the initial soliton radius and electromagnetic energy density. For $t/\tau \gg 1$, the postsoliton radius increases as $R \approx R_0(2t/\tau)^{1/3}$, and its amplitude and frequency decrease as $E \sim t^{-2/3}$ and $\omega_s \sim t^{-1/3}$.

A laser pulse, wider than a few times $d_e$, generates a cloud of solitons with conversion efficiency as high as $\kappa = 20\%$ according to the PIC results presented in Ref. [1]. The number $N_s$ of postsolitons depends both on the laser and on the plasma parameters. The laser pulse energy, normalized on $nm_ec^2$, can be written as $W = a^2 l_{\mathrm{pulse}} l_\perp^2$, where $a = eE/m\omega c$ is the dimensionless pulse amplitude and $l_{\mathrm{pulse}}$ and $l_\perp$ its length and width. The laser pulse loses its energy in the wake field and in the generation of solitons and quasistatic magnetic fields. Its depletion length is of the order of $l_{\mathrm{depl}} \approx l_{\mathrm{pulse}}(\omega/\omega_{pe})^2$. The volume traced by the pulse is approximately $l_{\mathrm{depl}} l_\perp^2$. The energy contained inside the soliton cloud is of the order of $W_{\mathrm{cloud}} = N_s d_e^3 a^2 = \kappa W$, with $d_e^3 a^2$ the characteristic energy of one soliton. Thus, the total number of solitons is $N = \kappa l_{\mathrm{pulse}} l_\perp^2 / d_e^3$. Assuming a uniform soliton distribution inside the volume traced by the laser pulse, we find the soliton density $n_s = \kappa (l_{\mathrm{pulse}}/l_{\mathrm{depl}})(1/d_e^3)$ and the intersoliton distance $D_s = d_e/[\kappa(l_{\mathrm{pulse}}/l_{\mathrm{depl}})]^{1/3} \approx d_e(\omega/\omega_{pe})^2$. Their expansion [2] makes the postsolitons merge after a time $t_b = \tau[l_{\mathrm{depl}}/(\kappa l_{\mathrm{pulse}})]$. Eventually they form a bubble much larger than the individual solitons. The bubble can even be larger than the volume traced by the laser pulse due to the soliton motion and to the expansion of the plasma as a whole.

The interpretation of the observed bubbles in terms of long-lived coherent structures resulting from postsoliton merging is supported by particle-in-cell simulations [11] that show that in plasma regimes where the density is not too small compared to the critical density, clouds of solitons are formed, evolve into expanding postsolitons, and eventually merge into bigger structures. This process can occur separately at different locations leading to separate

macrobubbles, e.g., around each filament if the laser pulse undergoes filamentation inside the plasma. The merging of two postsolitons is illustrated in Figs. 2a and 2b where the results of a 2D PIC simulation are presented for an $s$-polarized pulse with dimensionless amplitude $a = 1$, made of two parts of length $l_\parallel = 4\lambda$, width $l_\perp = 5\lambda$, and transverse distance $5\lambda$, in a plasma with density $n = 0.36n_{cr}$. Distances are measured in laser wavelengths $\lambda$ and times in laser periods $2\pi/\omega$. The pulse was initialized in such a way as to produce two spatially close solitons, as shown in Fig. 2a in the ion density distribution at $t = 90$. As the ions start to move and the two postsolitons expand, their walls intersect going through a transient merging phase that leads to the formation of a new almost circular shell, as shown in Fig. 2b at $t = 550$. A wider laser pulse with $a = 3$, length $l_\parallel = 15\lambda$, and width $l_\perp = 20\lambda$ in an underdense plasma with $n = 0.3n_{cr}$ generates a cloud of solitons. In Fig. 2c at $t = 140$ we see about 30 postsolitons formed after the laser pulse has filamented. As a result of the postsoliton merging, a big
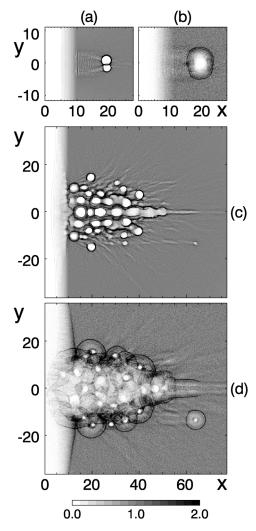


FIG. 2. Ion density distributions of two merging postsolitons during (a) and after (b) the merging process, as obtained from 2D PIC simulations. Ion density distribution in a cloud of merging postsolitons at $t = 140$ (c) and at $t = 550$ (d).

hole appears in the plasma density, as shown in Fig. 2d at $t = 550$. The evolution of the ion density shows that a macrobubble starts to form with a size of the order of the pulse depletion length, i.e., of the order of the size of the region inside which the solitons originally formed.

In the simulations of two postsoliton and multipost-soliton merging, the resulting structure evolves towards a nearly circular shape, i.e., the initial azimuthally inhomogeneous perturbation decays. This implies that the postsolitons are stable. Their stability can be proved analytically within the framework of the snowplow approximation [12,13]. In Ref. [14] the equations of mass conservation and of motion, under the effect of the ponderomotive pressure inside the postsoliton, are solved in the linear approximation in the case of an expanding cylindrical 2D postsoliton solution. A Fourier series in the azimuthal angle is adopted and the terms of this series, which describe the time evolution of the different azimuthal harmonic perturbations, are found to grow in time with a velocity smaller than that of the azimuthally symmetric equilibrium expansion for azimuthal mode numbers smaller than 6. This is in agreement with the numerical results shown in Fig. 2, if we take into account that the short wavelength modulations, not seen in Fig. 2, are expected to be stabilized by the finite width of the expanding shell which is not accounted for in the snowplow model. An analogous result is proved in Ref. [14] for the case of a spherical expansion.

In the single particle approximation, which applies when the Debye shielding of the electrons accompanying the probe proton beam occurs on a scale length larger than the bubble size, it is possible to find both the size of the bubble and the value of the quasistatic electric field inside from the observed proton image of the bubble. We recall that in the case of protons with $\approx 6$ MeV energy the effect of the oscillating electromagnetic field is averaged out during the proton transit time. The quasistatic electric field $E_{\parallel}$ inside the postsoliton is the order [2] of $E_{\parallel} \approx E_0(R_0/R)^4$, vanishes outside the cavity, and is directed normally to its walls. We assume that the postsoliton has a spherical shape and that the $E_{\parallel}$ has a linear spatial dependence $E_{\parallel} = E_{\parallel 0}(r/R)$. The transverse momentum gained from $E_{\parallel}$ by a proton crossing with velocity $v_z$ and impact parameter $r_0$ a bubble of radius $R$ is given by $\Delta p_{\perp} \approx (2eE_{\parallel 0}r_0/v_z)\sqrt{1 - r_0^2/R^2}$ for $r_0 < R$ and $\Delta p_{\perp} = 0$ for $r_0 > R$. The resulting proton density distribution at the distance $Z$ from the bubble located at a distance $Z_s < Z$ from the pointlike proton source, as shown in Fig. 3, is approximately constant inside the radius $r_1 = R(1 + Z/Z_s)$, i.e., inside the geometrical projection of the bubble on the image plane, has a jump at $r_1$, and tends to infinity at $r_2$. For relatively small deflections, $r_2 = r_1 + \delta r$ with $\delta r \approx (r_1/2)(eE_{\parallel 0}Z_s/m_p v_z^2)^2$. From the central bubble we can estimate $\delta r \approx 0.3r_1$ with $r_1 \approx 530$ $\mu$m. For $m_p v_z^2/2 = 6$ MeV, with $Z = 2$ cm
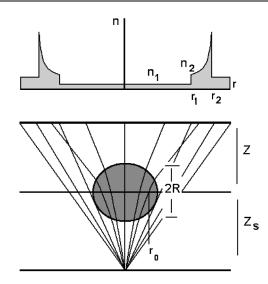


FIG. 3. Geometry of the proton deflection by the electric field in a postsoliton of radius $R$ at distance $Z_s$ from the proton source.

and $Z_s = 2$ mm, we obtain $E_{\parallel 0} \approx 4 \times 10^7$ V/cm, $R \approx 50$ $\mu$m.

In conclusion, we have shown that proton imaging allows us to detect long-lived, macroscopic electric field structures in the plasma. These bubblelike features can be consistently interpreted as originating from relativistic electron solitons that have been created in the plasma by the laser pulse and that have evolved into larger structures, due to expansion and merging under the effect of the ion dynamics discussed in Ref. [2].

[1] S. V. Bulanov *et al.,* Phys. Rev. Lett. **82**, 3440 (1999); Y. Sentoku *et al.,* Phys. Rev. Lett. **83**, 3434 (1999).
[2] N. M. Naumova *et al.,* Phys. Rev. Lett. **87**, 185004 (2001).
[3] M. Borghesi *et al.,* Plasma Phys. Controlled Fusion **43**, A267 (2001).
[4] R. D. Snavely *et al.,* Phys. Rev. Lett. **85**, 2945 (2000).
[5] E. L. Clark *et al.,* Phys. Rev. Lett. **84**, 670 (2000).
[6] A. J. Mackinnon *et al.,* Phys. Rev. Lett. **86**, 1769 (2001).
[7] M. Borghesi *et al.* (to be published).
[8] W. L. C. McLaughlin *et al.,* Nucl. Instrum. Methods Phys. Res., Sect. A **302**, 165 (1991).
[9] R. A. London and M. D. Rosen, Phys. Fluids **29**, 3813 (1986).
[10] M. Borghesi *et al.,* Proc. SPIE Int. Soc. Opt. Eng. **4424**, 414 (2001); M. Galimberti *et al.,* Proc. SPIE Int. Soc. Opt. Eng. **4424**, 512 (2001).
[11] T. Zh. Esirkepov, Comput. Phys. Commun. **135**, 144 (2001).
[12] E. Ott, Phys. Rev. Lett. **29**, 1429 (1972).
[13] S. V. Bulanov *et al.,* Phys. Rev. E **59**, 2292 (1999).
[14] S. V. Bulanov and F. Pegoraro (to be published).